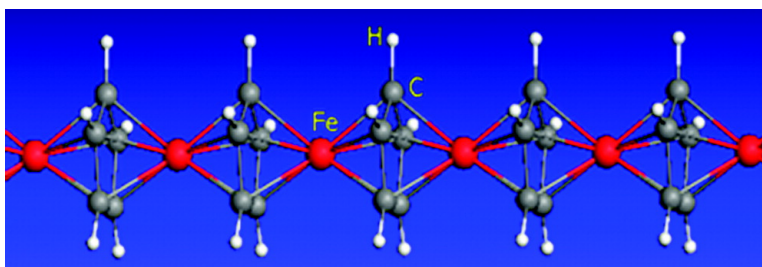Article

One-Dimensional Iron–Cyclopentadienyl Sandwich Molecular Wire with Half Metallic, Negative Differential Resistance and High-Spin Filter Efficiency Properties

Liping Zhou, Shuo-Wang Yang, Man-Fai Ng, Michael B. Sullivan, Tan, and Lei Shen

More About This Article

Additional resources and features associated with this article are available within the HTML version:

- Supporting Information
- Links to the 2 articles that cite this article, as of the time of this article download
- Access to high resolution figures
- Links to articles and content related to this article
- Copyright permission to reproduce figures and/or text from this article

View the Full Text HTML

One-Dimensional Iron−Cyclopentadienyl Sandwich Molecular Wire with Half Metallic, Negative Differential Resistance and High-Spin Filter Efficiency Properties

Liping Zhou,[†] Shuo-Wang Yang,*,[†] Man-Fai Ng,[†] Michael B. Sullivan,[†] Vincent B.C. Tan,[‡] and Lei Shen[†,§]

Institute of High Performance Computing, 1 Science Park Road, #01-01 The Capricorn, Singapore 117528, Singapore, Department of Mechanical Engineering, National University of Singapore, Singapore 117576, Singapore, and Department of Physics, National University of Singapore, Singapore 117542, Singapore

Received November 5, 2007; E-mail: yangsw@ihpc.a-star.edu.sg

Abstract: We present a theoretical study on a series of novel organometallic sandwich molecular wires (SMWs), which are constructed with alternating iron atoms and cyclopentadienyl (Cp) rings, using DFT and nonequilibrium Green's function techniques. It is found that that the SMWs are stable, flexible structures having half-metallic (HM) properties with 100% negative spin polarization near the Fermi level in the ground state. Some SMWs of finite size show a nearly perfect spin filter effect (SFE) when coupled between ferromagnetic electrodes. Moreover, their $I−V$ curves exhibit negative differential resistance (NDR), which is essential for certain electronic applications. The SMWs are the first linear molecules with HM, high SFE, and NDR and can be easily synthesized. In addition, we also analyze the underlying mechanisms via the transmission spectra and spin-dependent calculations. These findings strongly suggest that the SMWs are promising materials for application in molecular electronics.

Introduction

Currently, molecular electronics and spintronics have been attracting scientists' attention since conventional silicon-based microelectronics is likely to reach its limit of miniaturization by the laws of physics.[1] Meanwhile, certain linear molecular wires that possess unique electrical and magnetic properties have been studied enthusiastically since they are promising components for next-generation electronic devices, especially in high-density storage and quantum computing.[2] Among them, vanadium−benzene multidecker molecules (V_nBz_{n+1}) have been extensively studied due to their fantastic half-metallic and spin filter effects.[3−7] V_nBz_{n+1} is one of a few sandwich linear molecules or quantum lines that has been synthesized. However, the ferrocene analogues to this system with alternating iron atoms and cyclopentadienyl (Cp) rings have not been well studied. The $[Fe(C_5H_5)]_n$ sandwich molecular wires (SMWs) have been synthesized in the gas phase and characterized by

mass spectroscopy.[8] Furthermore, Kruse et al.[9] constructed highly ordered ferrocene molecular lines (HOFMLs) on H−Si (100) surface via a self-directed growth process. Therefore, as compared to the multidecker molecules (V_nBz_{n+1}), the SMWs should be easily realized with an appropriable template via a self-assembly process on surfaces and thus allow wide use in future devices.

Results and Discussion

In this paper, we study the structures, electron densities of states (DOS), band structures, spin polarizations, spin filter effects, and current−voltage ($I−V$) curves of the $[Fe(C_5H_5)]_n$ SMWs. We find SMWs are stable regardless of their configurations: eclipsed or staggered. The infinite linear SMWs, i.e., $[Fe(C_5H_5)]_n$ ($n \rightarrow \infty$), are one-dimensional half-metallic (HM)[10] in its ground state. Meanwhile, certain SMWs with finite size show a perfect magnetic spin filter effect (SFE) when coupled between ferromagnetic electrodes such as Fe or Ni. To our best knowledge, very few linear molecules possess both of the above-mentioned properties. Moreover, the $I−V$ curves of SMWs exhibit negative differential resistance (NDR), which is the defining behavior in several electronic components including Esak diode[11] and most notably resonant tunneling diodes.[12]

[†] Institute of High Performance Computing.
[‡] Department of Mechanical Engineering, National University of Singapore.
[§] Department of Physics, National University of Singapore.

(1) Ventra, M. D.; Pantelides, S. T.; Lang, N. D. *Phys. Rev. Lett.* **2000**, *84*, 979.
(2) Long, N. J. *Metallocenes*; Blackwell Science Press: Oxford, 1998.
(3) Miyajima, K.; Nakajima, A.; Yabushita, S.; Knickelbein, M. B.; Kaya, K. *J. Am. Chem. Soc.* **2004**, *126*, 13202.
(4) Wang, J.; Acioli, P. H.; Jellinek, J. *J. Am. Chem. Soc.* **2005**, *127*, 2812.
(5) Xiang, H.; Yang, J.; Hou, J. G.; Zhu, Q. *J. Am. Chem. Soc.* **2006**, *128*, 2310.
(6) Maslyuk, V. V.; Bagrets, A.; Meded, V.; Arnold, A.; Evers, F.; Brandbyge, M.; Bredow, T.; Mertig, I. *Phys. Rev. Lett.* **2006**, *97*, 097201.
(7) Koleini, M.; Paulsson, M.; Brandbyge, M. *Phys. Rev. Lett.* **2007**, *98*, 197202.

(8) Nagao, S.; Kato, A.; Nakajima, A. *J. Am. Chem. Soc.* **2000**, *122*, 4221.
(9) Kruse, P.; Johnson, E. R.; DiLabio, G. A.; Wolkow, R. A. *Nano Lett.* **2002**, *2*, 807.
(10) Groot, R. A. D.; Mueller, F. M.; Engen, P. G. V.; Buschow, K. H. J. *Phys. Rev. Lett.* **1983**, *50*, 2024.
(11) Sze, S. M. *Physics of Semiconductor Devices*, 2nd ed.; John Wiley and Sons: New York, 1981.
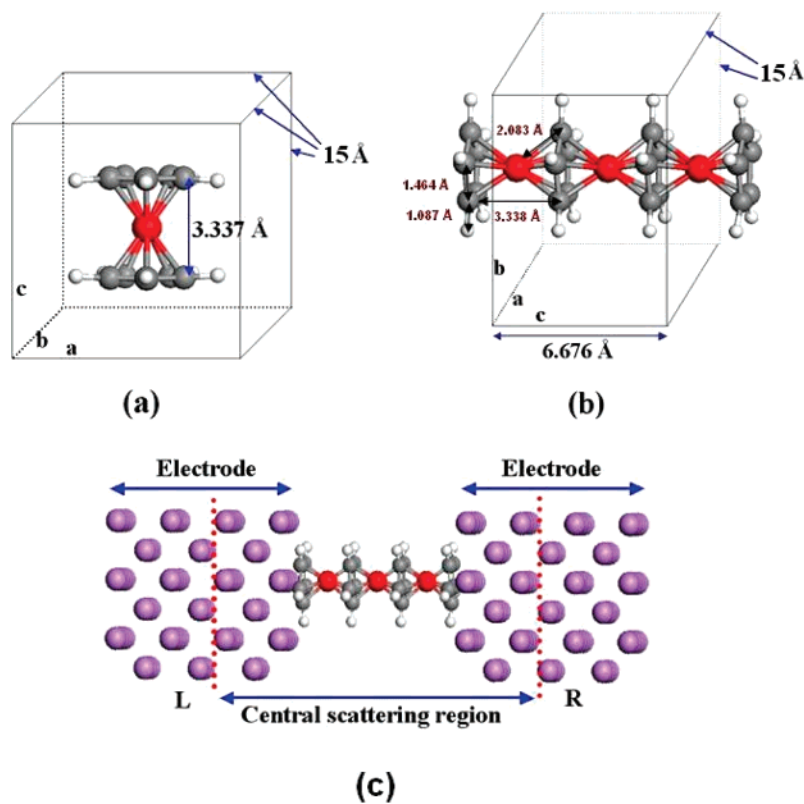
Figure 1. Structure optimization models (a) for a ferrocene molecule and (b) for the infinite SMW model with eclipsed configurations. Red spheres denote iron atoms, dark gray spheres denote carbon atoms, and small light gray spheres denote hydrogen atoms. (c) One-dimensional Fe_3Cp_4 SMW coupled between two lithium (001) surfaces of electrodes. The purpose of selection of Li as electrodes is to reduce computational cost. Vertical dotted lines represent borders of the central scattering region.

Therefore, our SMWs are the first unique linear molecules which possess HM, high SFE, and NRD simultaneously.

Structure optimizations and DOS calculations were performed using DMol3[13−15] and the Vienna ab initio simulation package (VASP)[16,17] for comparison. Figure 1a and b shows the models used for structure optimization, where a fixed $15 \times 15 \times 15$ Å unit cell with periodic boundary conditions is employed for the ferrocene molecule, an iron atom is positioned at the center of the cell, and two Cps are perpendicular to the longitudinal axis (z or c direction). The distance between the two Cps along the c direction in adjacent cells is about 11.7 Å to ensure that there is no interaction between neighboring cells (Figure 1a). While for the infinite SMW model the lattice parameters, a and b, are fixed at 15 Å, c, which is twice the distance between the Fe atom and the Cp ring, is optimized. For Dmol3 calculations, the generalized gradient approximation (GGA) schemes are used with Perdew−Burke−Ernzerhof (PBE) correlation functionals[18] and ultrasoft pseudopotentials[19] that are generated consistently. Special k points are generated according to the Monkhorst−Pack scheme for integration over the irreducible wedge of the Brillouin zone.[20] The calculated results of DMol3 are similar with VASP in DOS; therefore, we only present the DMol3 results in this paper.

The band structures, $I−V$ curves, and spin filter effects for several SMWs with eclipsed configurations and finite sizes are calculated with the ATOMISTIX TOOLKIT,[21−23] which combines DFT and nonequilibrium Green's function (NEGF) technique. PBE functionals were used with the non-spin-polarized GGA for the $I−V$ curve calculations, and spin-polarized GGA (SGGA) is applied for the spin filter calculations. Our calculations use a two-probe model shown in Figure 1c; the SMW is coupled between two (001) surfaces of bcc-Li or two (001) surfaces of fcc-Cu electrodes for the purpose of comparison. The Green's function and self-energies are calculated for the central region using the Landauer−Büttiker formula.[24] In all cases, the Cp rings are placed on top of the hollow sites of the electrodes surface, which is the same as in previous work.[6]

The optimized distance between the two Cp rings of the eclipsed ferrocene in the singlet ground state is the same as the experimental value (3.338 Å).[25] Again, the same value is obtained for the infinite SMW in its triplet ground state as shown in Figure 1b, where the geometry of the eclipsed SMW in its ground state is given. It is found that there is very little difference in the geometries for different spin states. Table 1 shows the bonding energies for the optimized systems at the

(12) Mathews, R. H.; Sage, J. P.; Sollner, T. C. L. G.; Calawa, S. D.; Chen, C.-L.; Mahoney, L. J.; Maki, P. A.; Molvar, K. M. *Proc. IEEE* **1999**, *286*, 596.
(13) Matsuzawa, N.; Seto, J.; Dixon, D. A. *J. Phys. Chem. A* **1997**, *101*, 9391.
(14) Delley, B. *J. Phys. Chem.* **1996**, *100*, 6107.
(15) Delley, B. *J. Chem. Phys.* **2000**, *113*, 7756.
(16) Kresse, G.; Hafner, J. *Phys. Rev. B* **1994**, *49*, 14251.
(17) Kresse, G.; Furthmüller, J. *Comput. Mater. Sci.* **1996**, *6*, 15.
(18) Perdew, J. P.; Burke, K.; Ernzerhof, M. *Phys. Rev. Lett.* **1996**, *77*, 3865.

(19) Vanderbilt, D. *Phys. Rev. B* **1990**, *41*, 7892.
(20) Monkhorst, H. J.; Pack, J. D. *Phys. Rev. B* **1976**, *13*, 5188.
(21) Brandbyge, M.; Mozos, J.-L.; Ordejón, P.; Taylor, J.; Stokbro, K. *Phys. Rev. B* **2002**, *65*, 165401.
(22) Soler, J. M.; Artacho, E.; Gale, J. D.; García, A.; Junquera, J.; Ordejón, P.; Sánchez-Portal, D. *J. Phys: Condens. Matter* **2002**, *14*, 2745.
(23) Taylor, J.; Guo, H.; Wang, J. *Phys. Rev. B* **2001**, *63*, 245407.
(24) Büttiker, M.; Imry, Y.; Landauer, R.; Pinhas, S. *Phys. Rev. B* **1985**, *31*, 6207.
(25) Haaland, A. *Top. Curr. Chem.* **1975**, *53*, 1.

Table 1. Bonding Energies of Ferrocene and SMWs at Different Configurations and Spin States

system	configuration	spin state	bonding energy (eV/Fe)
ferrocene (FeCp$_2$)	eclipsed	singlet	−4.20
	staggered	singlet	−4.18
SMW ((Fe$_2$Cp$_2$)$_n$)	eclipsed	singlet	−4.75
		triplet	−4.92
		quintet	−4.32
	staggered	singlet	−4.72
		triplet	−4.87
		quintet	−4.27

various spin states. The eclipsed configurations are nearly isoenergetic with the staggered ones.

Figure 2 shows the spin-polarized DOS and band structures at the ground state to compare SMWs to the V$_n$Bz$_{n+1}$ system. The DOS of staggered and eclipsed configurations are almost the same near the Fermi level, which further confirms that the rotation of the Cp rings has little effect on the electronic properties of SMWs, and we will only focus on the eclipsed SMW in the following calculations. The DOS of the SMW displays a striking feature of combining metallic (spin up) and semiconducting gap (spin down) at different spin channels and shows 100% spin polarization near the Fermi level (Figure 2a), indicating that it is half-metallic. According to our calculations, the eclipsed SMW with a bonding energy of 4.92 eV is more stable than V$_n$Bz$_{n+1}$ (4.01 eV in bonding energy).

Analysis of the band structure should be helpful in understanding the formation of the half-metallic feature. Figure 2b shows the spin-resolved band structures of the eclipsed SMW at the triplet spin state. The spin-up electrons (solid lines) are the majority electrons, and the spin-down (dot lines) electrons are the minority. According to crystal field theory, the eclipsed SMW has D_{5h} symmetry and the Fe 3d orbitals are split into a d$_{3z^2-r^2}$ orbital and two sets of doubly degenerate d$_{xy}$, d$_{x^2-y^2}$ and d$_{xz}$, d$_{yz}$ orbitals, which correspond to the three completely spin split bands in the band structure near Fermi level labeled as 1, 2, and 3, respectively. Three minority electrons fully occupy bands 1 and 2, opening a gap of about 2.2 eV at Γ point for the spin-down state as shown in the DOS. For the five spin-up electrons, one fully occupies the d$_{3z^2-r^2}$ orbital at −1.8 eV (band 1) and two others fill completely the d$_{xy}$ and d$_{x^2-y^2}$ orbitals at −1.0 eV (band 2). The remaining two spin-up electrons partially occupy d$_{xz}$ and d$_{yz}$ orbitals, which hybridize with the p orbitals of the Cp rings and remain at 1.8 eV (band 3). Band 3 for spin up crosses the Fermi level, indicating metallic property. Therefore, SMWs will have 100% negative spin polarization, similar to that of Fe$_3$O$_4$,[26] and contribute 2.0 μB magnetic moments per unit cell.

We used I−V curves as a way to study the electrical transport properties of SMWs. Figure 3 shows calculated I−V curves for various lengths of SMWs, namely, ferrocene (FeCp$_2$), Fe$_2$Cp$_2$, and Fe$_3$Cp$_4$ coupled between the Li electrodes. We can see that the shapes of the I−V curves correspond to the point symmetry of the molecules. For example, only the Fe$_2$Cp$_2$ structure shows an asymmetric I−V curve since it has no point of symmetry. Meanwhile, a linear region is found within a low electrical bias of ±0.6 V for both ferrocene and the SMWs. Striking negative differential resistance (NDR) features appear around 1 eV electrical bias. This behavior has gained widespread interest

since the NDR is necessary for several electronic components such as the Esaki and resonant tunneling diodes.[11,12] Most of the reported molecules that possess the NDR are very sensitive to geometrical factors such as the symmetry and length[27,28] and thus limit their applicability. In contrast, the NDR of SMWs is not affected by their configurations, and they show promise for molecular electronics.

To further understand the mechanism of the NDR, the transmission spectra of the Fe$_3$Cp$_4$ wire at zero and four different biases are studied, and the results are shown in Figure 4. Three significant transmission peaks, P1, P2, and P3, can be seen near the Fermi energy. Our calculations show that the HOMO and LUMO of the Fe$_3$Cp$_4$ wire are generated at the same energy level, giving rise to the P1 peak when the wire is coupled to the electrodes. Meanwhile, LUMO+1 and LUMO+2 give rise to the P2 and P3 peaks, respectively. We indicate the molecular projected self-consistent Hamiltonian (MPSH)[21−23] with green triangles. Two MPSH eigenvalues around 0.0 and 0.7 eV, labeled E_1 and E_2, respectively, are obtained at zero bias, and their values change with applied bias. Since they are affected by the frontier molecular orbitals, they are found around the E_F and give rise to three transmission peaks in the bias window. The spatially resolved wave functions show that E_1 and E_2 are mainly formed between the hybrid orbitals of Fe d$_{xz}$ and d$_{yz}$ orbitals and the Cp rings (Figure 4b).

It can be seen that when the voltage increases, the P1 peak shifts away from the Fermi level to the negative field with decreasing amplitude, especially at high bias. Meanwhile, the P2 and P3 peaks shift down to the Fermi level gradually and the amplitude of the P2 peak becomes smaller while the P3 peak gets bigger. At around 1.0 V, the P2 peak shifts into the bias window completely and is very small, leading to an abrupt decrease in the electrical current. As the bias further increases, the P3 peak becomes broader and moves further into the bias window, resulting in an increase of current and indicating the NDR effect. In this process, the P1 peak plays an important role in the conductance, but it is the competition between the P2 and P3 peaks that causes the NDR. The wavefunctions of the MPSH states of E_1 and E_2 at zero bias and at a bias of 2.0 V as shown in Figure 4b further validate this. The E_1 state changes very little, but the E_2 state shows very different symmetry at the different bias conditions; this implies the competition between the P2 and P3 transmission peaks along the bias change.

To further evaluate the NDR effect of the Fe$_3$Cp$_4$ molecule, we also calculated its I−V curve using the Cu electrodes, and the result is shown in the inset of Figure 3. As compared to the Li electrodes, the NDR appears at higher bias (2.5 eV), i.e., a larger current peak to valley ratio results. This is because the electron excitation energies for the Cu electrodes are larger than that of Li. The NDR for the Fe$_3$Cp$_4$ molecule is an intrinsic property and independent of the electrodes used. Gorman et al.[29] detected a similar NDR in ferrocenyl−undecanethiolate (Fc−C$_{11}$S−), which is self-assembled monolayer (SAM) prepared on a Au(111) surface. They proposed that the ferrocenyl groups are the actual fragment giving rise to the NDR. Our calculations confirm their assumption.

(26) Groot, R. A. D.; Buschow, K. H. J. *J. Magn. Magn. Mater.* **1986**, *54*, 1377.

(27) Hu, Y.; Zhu, Y.; Gao, H.; Guo, H. *Phys. Rev. Lett.* **2005**, *95*, 156803.
(28) Crljen, Z.; Grigoriev, A.; Wendin, G.; Stokbro, K. *Phys. Rev. B* **2005**, *71*, 165316.
(29) Gorman, C. B.; Carroll, R. L.; Fuierer, R. R. *Langmuir* **2001**, *17*, 6923.
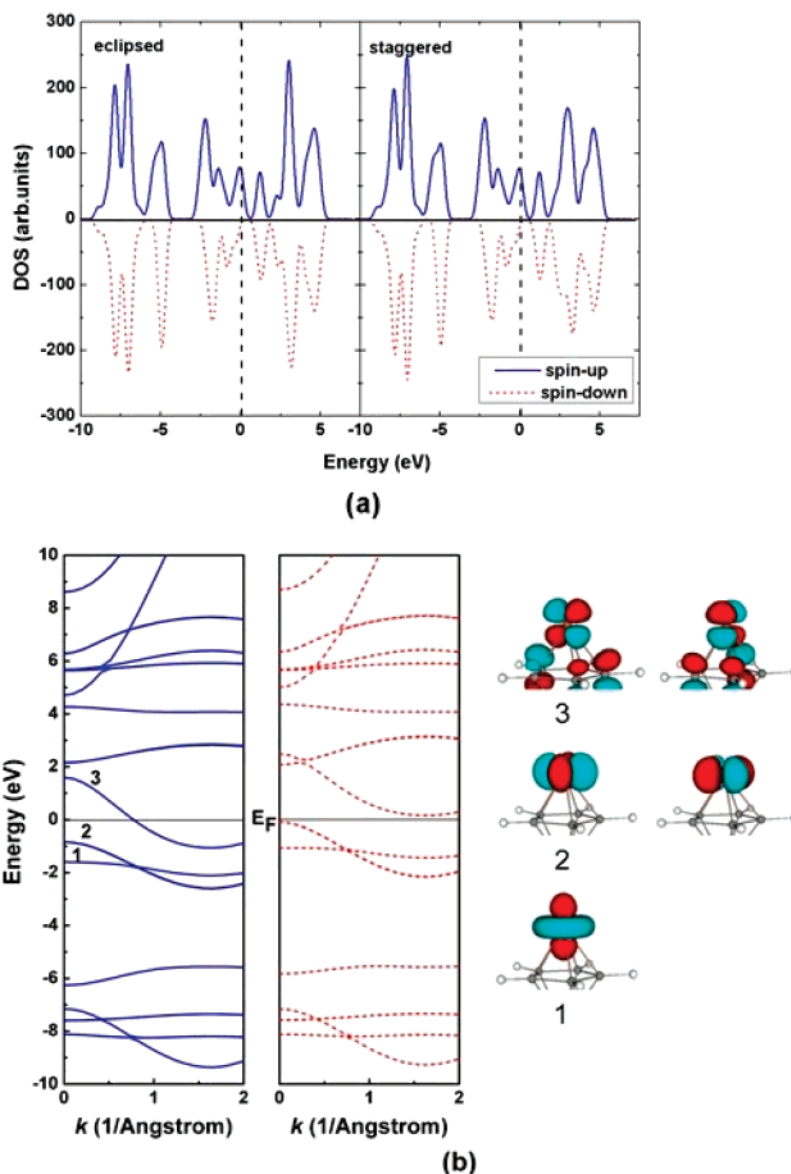
Figure 2. (a) Spin-polarized DOS and (b) spin-polarized band structure for eclipsed SMW at its ground state. The solid lines denote the spin-up electrons and dotted lines for the spin-down electrons. The crystalline orbitals are calculated at Γ point.
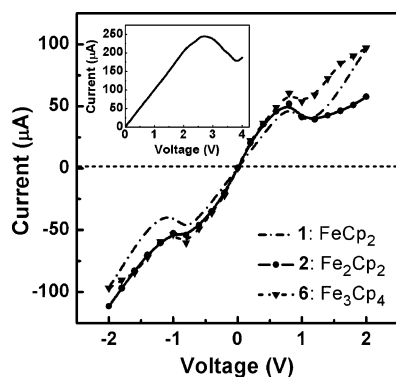

Figure 3. $I-V$ curves for eclipsed ferrocene and two SMWs coupled between two Li electrodes. The inset figure shows the $I-V$ curve of Fe$_3$-Cp$_4$ coupled between two Cu electrodes.

Finally, we perform spin-polarized calculations to investigate the spin-dependent transport of the SMWs with different lengths and contacts when coupled between the iron electrodes. Seven

SMWs, **1**−**7**, were selected for the calculations, and results are given in Table 2 and Figure 4c. It can be seen that around the Fermi level the transmission spectra for spin-up and spin-down channels are clearly separated, indicating again that it is half-metallic. While most of the SMWs show a good spin filter effect (SFE), the efficiency is strongly affected by the wire−electrode contacts. The unsymmetric SMWs, where one end is a Cp ring and the other end is a Fe atom, show the best SFE. For instance, the SMWs **2** and **5** show nearly perfect SFE with efficiencies approaching 100%. The SMWs with Fe atoms at both ends also show good SFE such as **4** and **7** wires. The SMWs with Cp rings at both ends (**1**, **3**, and **6**) perform quite poorly. We believe that the different contacts affect the strength of coupling of SMWs to the electrodes, which may influence the spin ground states and spin splitting so that their SFE would fluctuate. In addition, we also calculate the SFE of SMW **5** using Ni as the electrode; the efficiency of SMW **5** using a Ni electrode is very high (93.6%), demonstrating that SMWs' structures and the nature of the contact are more important than the electrodes.
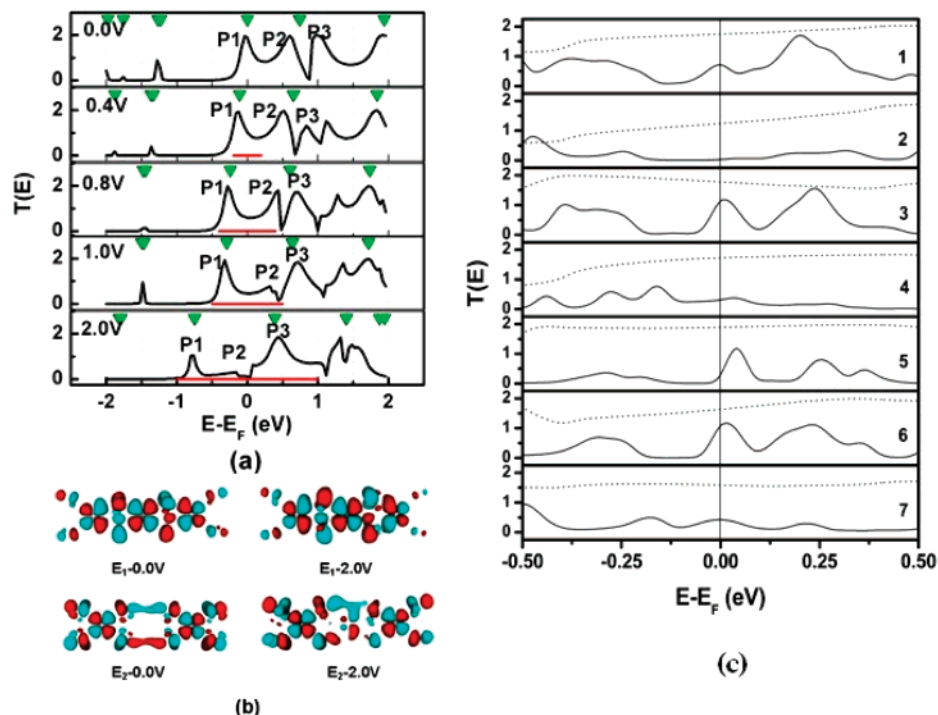
Figure 4. (a) Transmission spectra of Fe_3Cp_4 coupled between lithium electrodes at various electrical biases. The red lines denote the bias windows, and green triangles are molecular projected self-consistent Hamiltonian (MPSH) eigenvalues. (b) Wavefunctions of the MPSH state with energy E_1 and E_2 at 0 and 2.0 V. (c) Energy-dependent spin-polarized transmission spectra for seven eclipsed SMWs coupled between Fe electrodes. In each panel, the dashed lines denote the transmissions for spin-up electrons and the solid lines are for spin down. Here, the spin filter efficiency is defined as the spin-polarized electron current at the Fermi level: $[T(E_F)_\uparrow - T(E_F)_\downarrow]/T(E_F)_\uparrow$.

Table 2. Spin-Dependent Conductance and SFE for Seven SMWs When Coupled between Fe Electrodes

	configuration	conductance[a] (G)		spin filter efficiency (%)
		spin up	spin down	
1	$FeCp_2$	67.57	34.54	45.9
2	Fe_2Cp_2	48.01	0.89	98.1
3	Fe_2Cp_3	69.00	55.92	19.0
4	Fe_3Cp_2	66.76	11.37	83.0
5	Fe_3Cp_3	73.14	0.81	99.0
6	Fe_3Cp_4	63.08	52.26	17.2
7	Fe_4Cp_3	61.46	17.74	71.1

[a] The equilibrium conductance (G), i.e., at zero-bias condition, is evaluated by the transmission coefficient $T(E)$ at Fermi energy (E_f) of the system: $G = (2e^2)/(h)T(E_f)$, where e is electron charge and h is Planck's constant.

In addition, we notice that the spin-down channels have lower conductance compared to the spin-up channels for all SMWs investigated because the mechanism of conductance for the two channels is different; spin-up channels are metallic, but spin-down channels are semiconducting. The transmission spectra in Figure 4c show that quantum tunneling effects are important for electron transport of spin-down channels. Those SMWs that have shown excellent SFE are actually tunneling forbidden for

the spin-down channels at equilibrium. However, it is clear that the transmission spectra are electrical bias dependent. Therefore, different SFE will appear when an extra bias is applied. These characteristics as the bias changes deserve further study.

Conclusion

In summary, we investigated unique linear Cp−Fe sandwich molecules by DFT and NEGF techniques. We found that SMWs are stable and flexible structures, allowing free rotation of Cp rings. They show HM features at the ground spin state, and at the same time, certain systems show perfect SFE, which is very important for the electronics industry. Moreover, the calculated I−V curves show SMWs possess NDR, which is essential for state-of-the-art electronic applications. To our knowledge, the SMWs presented here are the first linear molecules with all three: HM, high SEF, and NDR. No doubt, they will be further studied by both theory and experiment.